LA-UR-15-28444
Approved for public release; distribution is unlimited.

Title: Aqueous Solution Vessel Thermal Model Development II

Author(s): Buechler, Cynthia Eileen

Intended for: Report

Issued: 2015-10-28

Cynthia Buechler **Aqueous Solution Vessel Thermal Model Development II** Oct. 6, 2015

Introduction

The work presented in this report is a continuation of the work described in the May 2015 report, "Aqueous Solution Vessel Thermal Model Development"[1]. This computational fluid dynamics (CFD) model aims to predict the temperature and bubble volume fraction in an aqueous solution of uranium. These values affect the reactivity of the fissile solution, so it is important to be able to calculate them and determine their effects on the reaction. Part A of this report describes some of the parameter comparisons performed on the CFD model using Fluent. Part B describes the coupling of the Fluent model with a Monte-Carlo N-Particle (MCNP) neutron transport model.

The fuel tank geometry is the same as it was in the May 2015 report, annular with a thickness-to-height ratio of 0.16. An accelerator-driven neutron source provides the excitation for the reaction, and internal and external water cooling channels remove the heat. The model used in this work incorporates the Eulerian multiphase model with lift, wall lubrication, turbulent dispersion and turbulence interaction. The buoyancy-driven flow is modeled using the Boussinesq approximation, and the flow turbulence is determined using the k-ω Shear-Stress-Transport (SST) model. The dispersed turbulence multiphase model is employed to capture the multiphase turbulence effects.

Part A. CFD Model Parameter Comparisons

Mesh – Edge Sizing

Several multiphase physics models have been added to the Eulerian multiphase model since the initial mesh checks were performed. This recent mesh study was performed to confirm that the model provides results that are mesh-independent and also to guide the choice of mesh size to use for other parameter studies. Calculations were performed using the geometry with 12 in-vessel cooling structures. Meshes were generated for a range of edge size, which is the approximate size of the hexahedral element edge on the outer surface of the vessel in the azimuthal direction. The edge length of the elements in the axial direction was 8 mm. The mesh parameters are listed in Table 1 along with the resulting volume-average temperatures (highlighted). A calculation was also performed using a tetrahedral instead of a hexahedral mesh. The maximum edge length for the tetrahedral mesh was 5 mm.

Mesh Edge Size	Element type	Mesh Method	Size Control	Wall Inflation Layers	Nodes	Elements	Vol-avg temp (K)	Vol-avg temp (°C)
8 mm	Hexa-hedrons	Sweep	Sweep element size: 8 mm	1st layer height: 0.04 mm Max layers: 15 Growth rate: 1.3 Bottom wall: sweep Number of Divisions: 12 Sweep bias: 20	84594	73843	320.7	47.52
6 mm	Hexa-hedrons	Sweep	Sweep element size: 8 mm	1st layer height: 0.04 mm Max layers: 15 Growth rate: 1.3 Bottom wall: sweep Number of Divisions: 12 Sweep bias: 20	99636	88365	320.7	47.51

[1] Buechler, Aqueous Solution Vessel Thermal Model Development, LA-UR-15-23537.

5 mm	Hexa-hedrons	Sweep	Sweep element size: 8 mm	1st layer height: 0.04 mm Max layers: 15 Growth rate: 1.3 Bottom wall: sweep Number of Divisions: 12 Sweep bias: 20	114402	102476	320.6	47.43
4 mm	Hexa-hedrons	Sweep	Sweep element size: 8 mm	1st layer height: 0.04 mm Max layers: 15 Growth rate: 1.3 Bottom wall: sweep Number of Divisions: 12 Sweep bias: 20	144762	131794	320.5	47.38
3 mm	Hexa-hedrons	Sweep	Sweep element size: 8 mm	1st layer height: 0.04 mm Max layers: 15 Growth rate: 1.3 Bottom wall: sweep Number of Divisions: 12 Sweep bias: 20	194994	180429	320.5	47.35
2 mm	Hexa-hedrons	Sweep	Sweep element size: 8 mm	1st layer height: 0.04 mm Max layers: 15 Growth rate: 1.3 Bottom wall: sweep Number of Divisions: 12 Sweep bias: 20	314916	295235	320.4	47.26
2 mm	Tetra-hedrons	Patch Conforming	Max Size: 5 mm	1st layer height: 0.04 mm Max layers: 15 Growth rate: 1.3 Bottom wall: patch conforming	287684	1033787	319.9	46.79

Table 1. Parameters and results of mesh edge-sizing study

The volume-average temperatures are all within 0.26°C of each other, except for the tetrahedral mesh, which was within 1°C of the hexahedral mesh results. The 6 mm edge size is judged to be sufficiently small to produce a quality hexahedral mesh.

Boussinesq Buoyancy Approximation

Another check performed was to verify that the results of the Boussinesq buoyancy approximation are still valid with the additional multiphase physics models enabled. All previous calculations assume a constant density of 1132 kg/m^3 and a thermal expansion coefficient of 0.00051 K^{-1}, which correspond to the reference temperature of 70°C. This temperature is higher than the steady-state values for the volume average temperature of the fuel, so for cases with steady-state temperatures closer to 50°C, the density is really 1143 kg/m^3 and the thermal expansion coefficient is 0.00045 K^{-1}. The thermal expansion coefficient of 0.00051 K^{-1} slightly overestimates the heat transfer. Volume average temperatures were calculated to be 47.26°C using the Boussinesq approximation and the hex mesh with 2 mm spacing. As shown in Table 2, this temperature result was just 0.33°C higher for the same problem using the temperature-dependent density.

Case	VolAve Density, Fuel (kg/m^3)	Vol-Ave Thermal Expansion Coefficient (K^{-1})	Min Density, Fuel (kg/m^3)	Max Density, Fuel (kg/m^3)	Max Temp (C)	Vol-Ave Temp (C)	Min Z-Veloc Fuel (m/s)	Max Z-Veloc Fuel (m/s)	Ave Fuel Vert Veloc (m/s)
Boussinesq	1132.0	0.000510	1132.0	1132.0	49.40	47.26	-7.19E-02	5.05E-02	-1.32E-02
Temp-dependent density	1144.6	0.000435	1143.5	1154.1	49.63	47.59	-7.00E-02	4.84E-02	-1.27E-02

Case	Max Vert Veloc Bubbles (m/s)	VolAve Vert Veloc Bubbles (m/s)	Max Vol Frac Bubbles	VolAve Vol Frac Bubbles	Energy balance (%)	h_Tave = Q/(A*(Tave-Tmid_wall), (W/m^2-K)	h_Tmax = Q/(A*(Tmax-Tmid_wall), (W/m^2-K)
Boussinesq	1.81E-01	1.29E-01	2.94E-02	8.62E-03	0.067	652.1	593.4
Temp-dependent density	1.78E-01	1.29E-01	2.88E-02	8.65E-03	-0.037	643.3	588.5

Table 2. Results of Boussinesq approximation compared to temperature-dependent density calculation

The downward velocities near the cold walls are larger for the Boussinesq approximation, because the thermal expansion coefficient is larger, and the natural convection flow that it produces is stronger. The strong downward flows at the walls entrain the bubbles longer, so the volume fractions are larger than they would be for the correct thermal expansion coefficient. We might expect to see an increased bubble volume fraction if the density had been underestimated, due to underestimated bubble velocity. However, this effect is secondary to the natural convection effects on the flow. The maximum vertical bubble velocity is slightly higher for the case using the Boussinesq approximation and the larger thermal expansion coefficient, and the volume average bubble volume fraction is slightly lower.

The Boussinesq approximation is valid for this flow problem and will be used for the calculations in the following sections. The average fuel density chosen for the constant-density material model is less important than the thermal expansion coefficient. Ignoring density effects, overestimating the thermal expansion coefficient[2] by 15% results in an overestimate of the heat transfer coefficient by just 1%. The temperature-dependent density may be used in the future if tracking the level height becomes important.

Transient Calculation

A transient calculation was performed using the hex mesh with 2 mm spacing to compare to the pseudo-transient (steady-state) calculation. Ten iterations are performed for each timestep in the transient calculation, so each timestep takes almost ten times as long as a pseudo-timestep in the pseudo-transient calculation. The steady-state

[2] At a temperature of 47.6°C.

results for the two calculation methods are nearly identical, as shown in Table 3. The pseudo-transient calculation method will be used for future calculations.

Case	Max Temp (C)	Vol-Ave Temp (C)	Min Z-Veloc Fuel (m/s)	Max Z-Veloc Fuel (m/s)	Ave Fuel Vert Veloc (m/s)
Pseudo-transient	49.40	47.26	-7.19E-02	5.05E-02	-1.32E-02
Transient	49.61	47.41	-7.24E-02	4.80E-02	-1.46E-02

Case	Max Vert Veloc Bubbles (m/s)	VolAve Vert Veloc Bubbles (m/s)	Max Vol Frac Bubbles	VolAve Vol Frac Bubbles	Energy balance (%)	h_Tave = Q/(A*(Tave-Tmid_wall), (W/m^2-K)	h_Tmax = Q/(A*(Tmax-Tmid_wall), (W/m^2-K)
Pseudo-transient	1.81E-01	1.29E-01	2.94E-02	8.62E-03	0.067	652.1	593.4
Transient	1.79E-01	1.29E-01	2.71E-02	8.62E-03	0.301	648.7	590.7

Table 3. Psuedo-transient (steady-state) calculation results compared to Transient calculation

Discretization Scheme and Multiphase Turbulence Model

Three other variations of this calculation were performed. The hex mesh with 6 mm spacing was used to reduce the time required to reach a steady-state result. The first of these variations involved changing the spatial discretization scheme for each of the flow variables from First Order Upwind to Second Order Upwind. Calculations tend to converge better with first-order discretization schemes, but increased accuracy may be achieved by using second-order discretization[3]. As seen in Table 4, the results change very little from the first to second-order discretization scheme. This is likely because the flow is aligned with the hexahedral mesh, so there is little numerical discretization error associated with the first-order discretization. The continuity residual, however, was two orders of magnitude higher for the second-order scheme than for the first-order.

In the second variation, the Quadratic Upwind Interpolation (QUICK) scheme was used for the spatial discretization, which is recommended for hexahedral meshes where unique upstream and downstream faces and cells can be identified[4]. This method uses a weighted average of Second Order Upwind and Central Differencing interpolation schemes to compute a higher-order value of the convected variable. The continuity residual for the QUICK calculation was an order of magnitude lower than it was for the first-order discretization scheme, and the calculation ran much faster. The volume-average temperature for the QUICK calculation was 0.1°C higher than for the first and second-order calculations.

[3] ANSYS FLUENT Users Guide, Section 28.2.1. First-Order Accuracy vs. Second-Order Accuracy.
[4] ANSYS FLUENT Theory Guide, Section 20.3.1.7 QUICK Scheme

Case	Max Temp (C)	Vol-Ave Temp (C)	Min Z-Veloc Fuel (m/s)	Max Z-Veloc Fuel (m/s)	Ave Fuel Vert Veloc (m/s)	Max Vert Veloc Bubbles (m/s)	VolAve Vert Veloc Bubbles (m/s)
First Order Upwind, Turbulence multiphase: Dispersed	49.42	47.26	-7.17E-02	4.78E-02	-1.38E-02	1.78E-01	1.29E-01
Second Order Upwind, Turbulence multiphase: Dispersed	49.62	47.26	-7.31E-02	5.11E-02	-1.34E-02	1.82E-01	1.29E-01
QUICK, Turbulence multiphase: Dispersed	50.05	47.36	-7.48E-02	5.43E-02	-1.34E-02	1.85E-01	1.29E-01
First Order Upwind, Turbulence multiphase: Per Phase	49.88	47.65	-7.47E-02	4.85E-02	-1.44E-02	1.79E-01	1.30E-01

Case	Max Vol Frac Bubbles	VolAve Vol Frac Bubbles	Energy balance (%)	h_Tave = Q/(A*(Tave-Tmid_wall), (W/m^2-K)	h_Tmax = Q/(A*(Tmax-Tmid_wall), (W/m^2-K)	Continuity residual
First Order Upwind, Turbulence multiphase: Dispersed	2.69E-02	8.74E-03	0.037	653.2	595.4	1.67E-05
Second Order Upwind, Turbulence multiphase: Dispersed	2.95E-02	8.62E-03	0.062	653.5	590.8	4.20E-03
QUICK, Turbulence multiphase: Dispersed	2.75E-02	8.66E-03	0.027	650.3	580.5	1.18E-06
First Order Upwind, Turbulence multiphase: Per Phase	2.89E-02	8.62E-03	0.040	642.0	584.4	3.69E-04

Table 4. Comparison of First and Second order discretization schemes and the Per-Phase turbulence multiphase model

The third variation involved changing the turbulence multiphase model from Dispersed to Per Phase, which is the recommended turbulence multiphase model for flows in which turbulence transfer between the phases produces a strong effect[5]. When the Per Phase model is selected, the SST k-ω model is applied to each phase. Using this model is more computationally intense than using the Dispersed model, as two additional transport equations must be solved for the secondary phase. As shown in Table 4, little difference is seen between the results.

The accuracy of the results may increase marginally using the second-order discretization scheme and the Per Phase turbulence multiphase model, but the calculation residuals also increase, indicating that the results are not as well converged. The QUICK scheme, however, is an efficient alternative to first-order discretization. It provides increased accuracy without a compromise in convergence. The first-order discretization scheme and the Dispersed turbulence multiphase model are used in the coupled calculations described in the next section, but future calculations will take advantage of the QUICK discretization scheme.

[5] ANSYS FLUENT Users Guide, Section 25.5.4. Modeling Turbulence.

Mesh – Inflation Layer Sizing

Lastly, the mesh inflation layer sizing near the walls of the vessel was examined. The size of the first-layer thickness used in the previous calculations was 40 µm. Meshes with first-layer thicknesses of 30, 20, and 10 µm were tested to verify that the results remained the same. The edge spacing used for the four calculations was 6 mm. The results exhibited almost no change and are compared in Table 5. The only notable difference in results is the maximum vertical velocity for the bubbles in the 10 µm case. With decreasing first-layer thickness, there is no change in maximum vertical bubble velocity until it jumps from 18 cm/s to 9.6 m/s for the 10 µm case. Although the volume average bubble velocity remains unaffected, this jump in maximum vertical velocity could indicate an instability due to poor mesh quality in some regions. The edge spacing used for the meshes stays constant while the thickness decreases, which can result in elements with extremely high aspect ratios. It is likely that the 10 µm first layer thickness produces a mesh of poor enough quality in some locations to affect the results. Calculations using the mesh with a 30 µm first layer thickness were found to converge the most quickly, so a 30 µm first layer thickness is used in the coupled Fluent-MCNP calculations, which will be described in the next section.

First-layer thickness	Max Temp (C)	Vol-Ave Temp (C)	Min Z-Veloc Fuel (m/s)	Max Z-Veloc Fuel (m/s)	Ave Fuel Vert Veloc (m/s)
40 µm	49.71	47.51	-7.19E-02	4.89E-02	-1.37E-02
30 µm	49.72	47.54	-7.17E-02	4.87E-02	-1.42E-02
20 µm	49.70	47.54	-7.15E-02	4.86E-02	-1.35E-02
10 µm	49.81	47.61	-7.18E-02	4.89E-02	-1.32E-02

First-layer thickness	Max Vert Veloc Bubbles (m/s)	VolAve Vert Veloc Bubbles (m/s)	Max Vol Frac Bubbles	VolAve Vol Frac Bubbles	Energy balance (%)	h_Tave = Q/(A*(Tave-Tmid_wall), (W/m^2-K)	h_Tmax = Q/(A*(Tmax-Tmid_wall), (W/m^2-K)
40 µm	1.79E-01	1.30E-01	2.96E-02	8.62E-03	-0.027	644.8	587.5
30 µm	1.79E-01	1.30E-01	2.99E-02	8.62E-03	-0.050	645.1	588.2
20 µm	1.79E-01	1.30E-01	2.77E-02	8.62E-03	-0.047	645.1	588.7
10 µm	9.6E-00	1.30E-01	3.05E-02	8.62E-03	0.040	643.1	586.1

Table 5. Parameters and results of mesh inflation layer sizing study

Part B. Coupled Fluent-MCNP Calculations

MCNP Calculation

The calculations described in the previous sections make use of a constant power profile determined by a single MCNP neutron transport calculation. The MCNP calculation determines the neutron interaction for the entire reactor system, not just the fuel vessel. It makes use of material libraries to determine the rate that neutrons from a defined source interact with each material. Interaction rates are converted to energy deposition rates and then used as the input for the Fluent calculation.

In the input file for the MCNP calculation, the entire 3-D geometry of the reactor system is defined. Only one cell is used to define the fuel volume, so average liquid densities and temperatures are defined for the fuel. The neutron calculation mode is specified, and fission cross-sections for both prompt and delayed neutrons are evaluated. The neutron source is defined as a thin vertical cylinder in the center of the reactor system. The probability density distribution for the neutron emission is weighted toward the mid-height region of the cylinder. Materials are specified for the fuel, tank walls, cooling water and all other reactor system components. Material libraries for Uranium-235, Uranium-238, hydrogen, oxygen, and sulfur are specified for the fuel, along with the atom fraction of each component. Temperatures are also specified for each cell.

The last part of the MCNP input file sets up the parameters for the requested results or tallies. A 3-D axially-symmetric mesh is specified, and the fissions are tallied for each mesh element. A single element is specified in the azimuthal direction, so the resulting mesh tally becomes a 2-D array of values. The specific tally requested for the mesh results is a cell flux tally with the fission reaction identifier, which returns the fission rate in each mesh cell[6]. MCNP normalizes all tallies to be the response for a single source particle, and it normalizes the cell flux tally by dividing by the volume, so the units[7] are returned as fissions/cm^3/source neutron. The final instruction in the MCNP input file specifies the number of particle histories to run for the calculation. The accuracy of the results improves with an increased number of particle histories.

The fission rates reported in the mesh tally output file are converted to energy deposition rates by multiplying by the source strength and the fission energy for Uranium-235. The source strength is an adjustable parameter for the system. It is determined by the settings used for the operation of the deuterium-tritium accelerator. The fission energy (3e-11 J/fission) is determined by multiplying the estimated thermal energy released in the fission of one Uranium-235 atom, (190 MeV/fission)[8] by the energy of one electron volt (1.6e-19 J/eV).

Sequential Fluent-MCNP Calculation Method

Up to this point, there has been no consideration of the effects that the fuel temperature and gas void fraction have on this power profile, but the power profile is actually coupled to the density of the fuel. The energy deposition is determined by the likelihood of a neutron interacting with a fuel molecule, and this likelihood increases with increased liquid density. The temperature and gas void fraction both contribute to the average density of the fuel, so

[6] X-5 Monte Carlo Team, MCNP — A General Monte Carlo N-Particle Transport Code, Version 5, Volume I: Overview and Theory, LA-UR-03-1987.

[7] The units for a plain F4 flux tally are tally-particles/cm^2/source-particle. A multiplier card is used to multiply the F4 flux tally by the atom density (atoms/cm^3) and reaction cross section (reactions·cm^2/atom/tally-particle). In this case, the tally and source particles are neutrons, and the reaction is specified to be fission, so the resulting units are fissions/cm^3/source neutron.

[8] LaMarsh, Introduction to Nuclear Engineering, 2nd Ed., p. 77. (190 MeV/fission is a low estimate. Table 3.6 lists the total recoverable energy for fission of U-235 as 198-207 MeV.)

a steady-state solution is only obtained when these effects are considered in the determination of the power profile. Another effect of temperature on the MCNP calculation is in the treatment of elastic scattering of low-energy neutrons. Again, at higher temperatures, interaction is less likely.

To account for these effects, a method has been developed to perform a series of sequential Fluent and MCNP calculations, as shown schematically in Figure 1. MCNP mesh tally results are used to define the internal heat generation profile in the reaction vessel. A Python program is used to couple the Fluent and MCNP calculations by automatically performing sequential iterations. An MCNP calculation is performed using an average fuel density, determined by the temperature and void fraction results from Fluent. The Fluent calculations are then updated using the MCNP mesh tally results for the internal heat generation profile. Iterations are repeated until changes in the power profile are small.

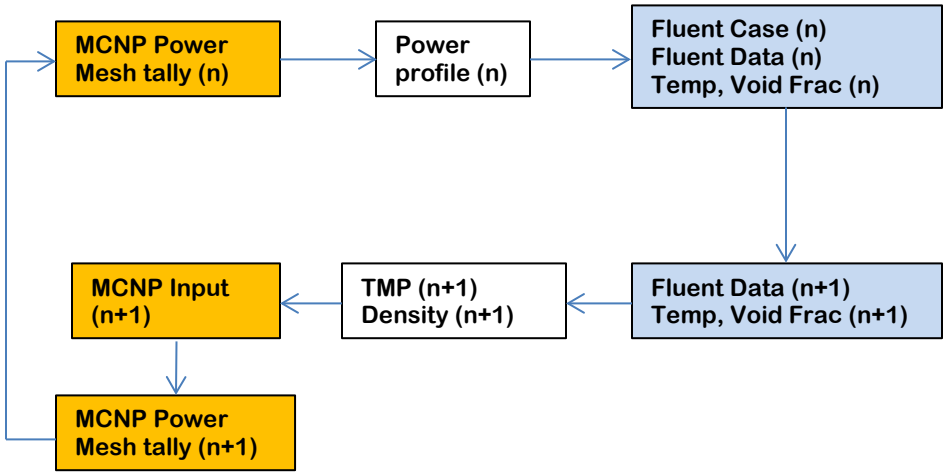

Figure 1. Schematic of sequential Fluent-MCNP calculation process

The detailed steps of the coupled calculation are listed below:

1. The case and data file from a converged Fluent calculation are placed in the working directory along with a mesh tally results file from an MCNP calculation.
2. The Python program is started, and it begins by converting the mesh tally data in a text file to a 2-D array of volumetric heating values, which is embedded in a user-defined function (udf) template.
3. A Fluent input file is generated with a list of commands for executing the calculation. The case and data file for the current iteration are specified, as well as the udf. The case file remains the same for each iteration, but the data file containing the results from the previous iteration is used to begin the current iteration. Instructions to unload the previous udf, then to compile and load the new udf are included. The last command initiates the calculation by specifying a number of iterations.
4. A command to execute Fluent using the current input file is sent to the computer node. The number of processors and the name of the output file are specified.
5. The Fluent calculation begins with the compiling and loading of the udf. A bi-linear interpolation function in the udf uses the 2-D array produced in step 2 to assign a volumetric heat and gas generation value to each cell in the 3-D domain. The axially-symmetric heat and gas generation profiles are constant throughout the Fluent calculation. Constant wall temperature profiles are also specified in the udf.
6. As the calculation progresses, monitor values are written to output files at each sub-iteration. Volume-average temperature, volume-average volume fraction, total integrated surface heat flux, and volume-integrated heat generation values are recorded.

7. The Python program displays the sub-iteration number every 15 seconds and checks to determine if the specified number of sub-iterations have completed. An exit command then instructs Fluent to write a case and data file and terminate the calculation.
8. The cleanup script that Fluent generates upon starting each calculation is identified in the working directory and executed to ensure that all of the Fluent processes are stopped and the licenses are released.
9. The data file for the completed iteration is identified among all of the data files in the working directory by referring to its time stamp. Its name is stored in order to be specified in the Fluent input file for the next iteration.
10. The final values in the volume-average temperature and volume-average volume fraction monitor output files are retrieved and used to calculate the equivalent fuel density for the next MCNP calculation. The final volume-integrated heat generation value is used to calculate the wall temperature profiles for the next Fluent iteration, and it is used to judge convergence of the coupled Fluent-MCNP calculation.
11. The current iteration number is appended to the output files to prevent them from being overwritten, and the iteration number is incremented.
12. An MCNP input file is created by updating a template with the current equivalent fuel density and temperature.
13. A command to execute MCNP using the current input file is sent to the computer node. The number of processors and the name of the output files are specified.
14. MCNP runs the specified number of particle histories, and the results for the fissions/cm^3/source neutron are written to a new mesh tally file. This file is used in the next iteration of the coupled calculation.

The liquid level height in both the Fluent and MCNP models remains constant throughout the iterations. To represent a level change caused by a change in fuel density and volume fraction, the geometry and mesh would need to be recreated for each Fluent iteration, and the surface representing the top of the fuel would need to be updated in MCNP. It may be possible to add this capability to future coupled calculations.

The un-coupled calculations presented in the previous sections have used a constant temperature of 25°C as the boundary condition on all of the tank walls, including the in-vessel cooling structures. To simulate the wall temperature increase that would occur for the case of cooling water entering the channels from the bottom and leaving on the top, the coupled calculations use a linearly-increasing temperature profile. The slope of this profile is a function of power level, and the total vessel power from the previous Fluent iteration is used to calculate the wall temperature profiles for the current iteration.

The vessel heat is removed by water cooling channels on the inner and outer surfaces of the annular tank as well as in-vessel cooling structures in the center of the tank. The wall temperature profile calculation assumes an inlet temperature of 20°C and an average water velocity of 0.56 m/s. The flow is divided among the individual channels according to cross-sectional area. The heat transfer coefficient for each cooling channel is estimated using the Dittus-Boelter correlation[9] for turbulent flow in cooling tubes. The temperature difference across the cooling channel boundary layer is determined using this heat transfer coefficient and assuming uniform heat flux over all cooled surfaces. This is added to the temperature difference across the thickness of the tank wall, constructed of Zircaloy-4. The bulk temperature rise of the cooling water from inlet to outlet is calculated based on the channel flow rate and uniform heat flux assumption. A single linear temperature profile from the bottom of the tank to the top is determined by averaging the linear profile for all wall surfaces. A scaling factor is applied to adjust the slope of this linear temperature profile according to power level.

[9] Incropera, Fundamentals of Heat and Mass Transfer, 4th Ed., p. 445.

Results of Coupled Fluent-MCNP Test Calculations

Four test calculations were performed and allowed to run for 17 sequential Fluent-MCNP iterations. The models used do not represent a unique physical reactor system but served the purpose of testing the code for convergence. Results are presented as normalized values.

The first calculation ran 50,000 sub-iterations for each Fluent iteration and 10,000 particle histories for each MCNP iteration. The total operating power at the end of each iteration is shown in Figure 2. The operating power is normalized to the initial power used at iteration 0. The steady-state operating power was calculated by averaging the power results for the last ten iterations (8-17). The percent difference from this steady-state operating power was calculated for each iteration and is displayed in Figure 3. By iteration 2, the percent difference is as low as it is in later iterations. Operating power results continue to bounce around ±5% of the steady-state value. Volume-average volume fraction results track with the operating power results at each iteration, as the gas-generation profile is just a scaled version of the heat generation profile.

To calculate the elastic scattering of low-energy neutrons, MCNP requires the temperature card (TMP in Figure 1) to be defined specifically for each cell. The first coupled Fluent-MCNP calculation was performed updating the TMP card in the MCNP input file at every iteration. To determine the significance of this temperature effect, the second coupled calculation was performed using a constant TMP value. The steady-state power results were about 6% lower with the constant TMP card, as shown in Figure 2. This is because the constant temperature maintained for the TMP card throughout the second calculation was almost 9°C higher than the steady-state fuel temperature at the end of the first coupled calculation. The higher temperature resulted in a decreased interaction rate and a lower steady-state power level. Again, the operating power results bounced around ±5% of the steady-state value.

The third coupled calculation was performed using 100,000 sub-iterations for each Fluent iteration and 100,000 particle histories for each MCNP iteration. This reduced oscillations in the power results to ±1% of the steady-state value.

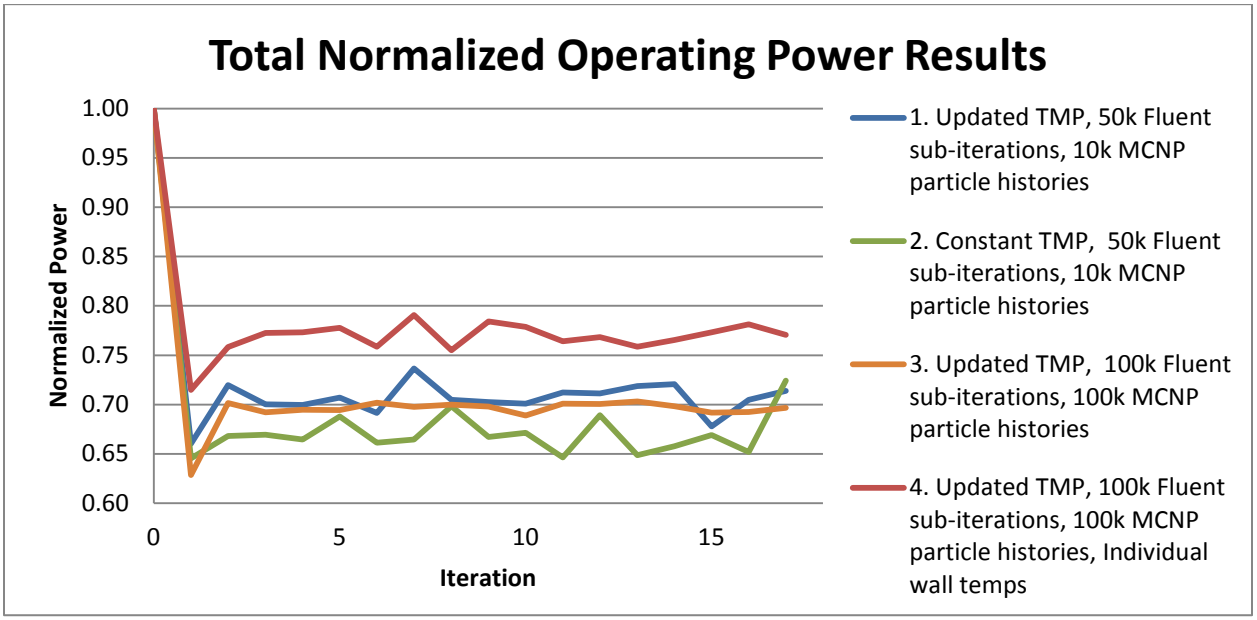

Figure 2. Operating power results at each iteration, normalized to the power used for iteration 0

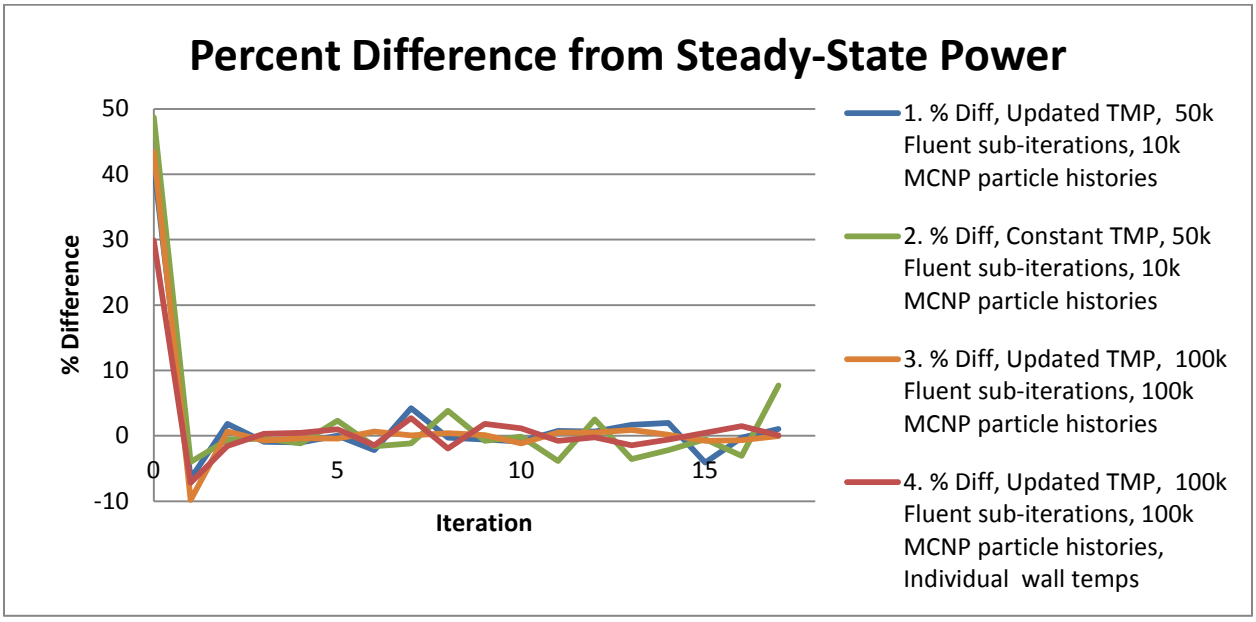

Figure 3. Percent difference between power result at each iteration and the average steady-state result

The first three coupled Fluent-MCNP calculations were performed using a single linearly-increasing temperature profile on all tank walls. The slope of this profile is a linear function of power level, with higher power levels resulting in a higher wall temperature at the top of the tank. However, the temperature at the bottom of the tank was not programmed to be a function of power level. The temperature at the bottom of the tank was defined to be a constant 33.7°C, which corresponds to a normalized power level of almost 1.3, much higher than the operating power at steady state. To accurately specify this boundary condition, the temperature at the bottom of the tank must be a function of power level. The temperature rise across the boundary layer in the cooling channel and the rise across the thickness of the metal wall both depend on the heat flux at these surfaces.

The fourth coupled Fluent-MCNP calculation includes linear power-dependence for the wall temperature at the bottom of the tank. Also, rather than assuming uniform heat flux on all walls, it uses average heat flux values for individual walls determined from preliminary calculations to specify the temperature profile function for each wall. The result of the function is applied to the boundary condition for the individual wall.

Again, 100,000 Fluent sub-iterations and 100,000 MCNP particle histories were used for the fourth coupled calculation. This calculation produced a steady-state operating power that was 10% higher than the third, due to the correction of the cold wall temperature at the bottom of the tank and the specification of individual temperature profiles on each of the cold walls. The operating power results bounced around ±2% of the steady-state value.

The result of this fourth coupled calculation is the best estimate of a steady-state operational mode for this subcritical reactor. The cold-start fuel level may be determined by subtracting the volume occupied by the gas bubbles from the steady-state fuel volume and then adjusting that volume back to room temperature. The average of the results for volume-average volume fraction of bubbles over the last 10 iterations for the fourth coupled calculation was 0.00655. This corresponds to a change in level height on the order of 1 cm from cold-start to steady-state.

Summary

The parameters for a CFD model of an accelerator-driven fissile solution system have been explored, and a preferred parameter set has been identified. The CFD model predicts the steady-state temperature and bubble volume fraction for the fuel in response to specified heat and gas generation profiles.

A method has been developed to calculate the steady-state temperature and bubble volume fraction that accounts for the coupled effects of these values on the heat and gas generation profiles. Sequential calculations are performed with resulting data being passed between the CFD and neutron transport models. A steady-state solution is achieved when the operating power level remains nearly constant. This coupled model can be used to predict the steady operation states and overall heat transfer coefficients for a variety of aqueous solution reactor systems.